Journal of Zhejiang University-SCIENCE A (Applied Physics & Engineering)
ISSN 1673-565X (Print); ISSN 1862-1775 (Online)
www.zju.edu.cn/jzus; www.springerlink.com
E-mail: jzus@zju.edu.cn

# Three-dimensional numerical simulation and earth pressure analysis on double-row piles with consideration of spatial effects

Zi-han WANG†, Jian ZHOU

(*Department of Geotechnical Engineering, Tongji University, Shanghai 200092, China*)

†E-mail: wangzihan1984@163.com

Received Feb. 15, 2011; Revision accepted July 13, 2011; Crosschecked Sept. 8, 2011

**Abstract:** As a new kind of technology in retaining structures, the characteristics of double-row piles are significantly affected by spatial effects. In this paper, double-row piles as a retaining structure are simulated numerically in three-dimension by finite element software PLAXIS 3D FOUNDATION. The behavior differences of piles in different positions around the foundation pit are analyzed. By changing the parameters, including the length-width ratio, the excavation depth, the distance between rows and the diameter of piles, the variations of the lateral deformation, the bending moment and the earth pressure around the piles are determined. The reasonable values of parameters and some suggestions with consideration of earth pressure are proposed for the design of double-row piles as a retaining structure. The results show that the lateral deformation and bending moment are the largest in the middle of long side of the foundation pit, which is identified as the most unfavorable position. It is indicated that the earth pressure between rows above pit bottom is close to active earth pressure, while the earth pressure between rows under pit bottom is close to static earth pressure. It is suggested that 1/2–2/3 of pile length, 0.6–1.2 m, 3*d*–6*d*, and 2*d*–2.5*d* be chosen as embedded depth of piles, diameter of piles, distance between rows, and distance between piles, respectively, where *d* is the pile diameter.

**Key words:** Double-row piles, Retaining structure, Spatial effect, Finite element, Earth pressure
**doi:**10.1631/jzus.A1100067 **Document code:** A **CLC number:** TU4

## 1 Introduction

As a new kind of technology in retaining structures, double-row piles have been produced by the China Academic of Building Research and Beijing Construction Engineering Group. The lateral stiffness of the retaining structures is enhanced due to spatial effects, the deformation produced by excavation is smaller with the comparison of the single-row piles as a retaining structure, and the lateral deformability resistance is greatly improved (Sun, 2008). Double-row piles as a retaining structure have been widely used in foundation engineering.

Based on laboratory model tests and engineering tests of double-row piles as a retaining structure, the model of a plane rigid frame (He *et al.*, 1996) is proposed, which has been widely used in practice. However, there is a greatly varying distribution of earth pressure between the front-row pile and the back-row pile in this model, which leads to deviation between practice and theory. A new model of a plane bar-system finite element, considering the interaction between the pile and soil (Zheng *et al.*, 2004), is proposed. The soil between rows is assumed to be thin-compressed layer that is simulated by horizontal springs. The earth pressure is distributed to piles by deformation coordination among the springs, the front-row pile, and the back-row pile. A part of double-row piles as a retaining structure is analyzed in three-dimension by finite element or finite difference software (Yang, 2005; Wu, 2006), and the internal force and deformation of retaining structures are analyzed. It is essential to perform real 3D

analyses on double-row piles as a retaining structure, being able to reflect the spatial effects on the whole foundation pit.

In this study, using finite element software PLAXIS 3D FOUNDATION, double-row piles as a retaining structure are simulated in real three-dimension, considering the spatial effects on the whole foundation pit. The behavior differences of piles in different positions around the foundation pit are analyzed. By changing the parameters, including the length-width ratio, the excavation depth, the distance between rows and the diameter of piles, the variations of the lateral deformation, the bending moment, and the earth pressure around the piles are determined. The reasonable values of parameters and some suggestions with consideration of earth pressure are put forward for the design of double-row piles as a retaining structure.

## 2 Finite element model

### 2.1 Establishment of the model

The software PLAXIS 3D FOUNDATION (Version 1.6) is used to establish the model. Considering the spatial effects and computing power of the computer, the size of foundation pit selected is 80 m ×40 m×10 m. The 1/4 of foundation pit is chosen to be the researching object due to the symmetry. The computational domain is 80 m×70 m×50 m, extending to 40–50 m outside foundation pit. The retaining structures are bored piles. The pile diameter, pile length, distance between piles, and distance between rows are 0.6, 18, 1.5, and 2.5 m, respectively.

The plane shape of model is shown in Fig. 1. The *X*-axis is along the long side of the foundation pit, pointing to the right. The *Z*-axis is along the short side of the foundation pit, pointing downwards. The *Y*-axis is perpendicular to the *X*-*Z*-plane, pointing towards the user. There are eight lines around the foundation pit to improve the mesh, which cannot affect the mechanical properties of model.

The soil is homogeneous. The constitutive model of the soil is Mohr-Coulomb (Neher *et al.*, 2001; Brinkgreve, 2002). The density is 19 kN/m$^3$; the elastic modulus is 40 MPa; Poisson's ratio is 0.35; the cohesion is 15 kN/m$^2$; the internal friction angle

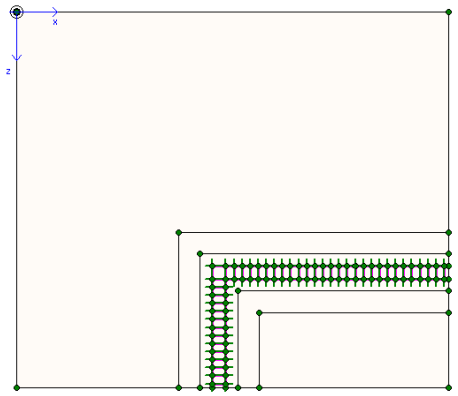

**Fig. 1 Plane shape of model**

is 20°; the interface-reduction coefficient is 0.7; and the dilatancy angle is not considered. The piles are simulated by changing the properties of soil in the same positions. The constitutive model is linear-elastic. The density is 25 kN/m$^3$; the elastic modulus is $2.5\times10^4$ MPa; and Poisson's ratio is 0.2. The coupling beams are simulated by linear-elastic beam elements. The section size is 0.8 m×0.8 m. The density is 25 kN/m$^3$; the elastic modulus is $3\times10^4$ MPa; and Poisson's ratio is 0.2.

PLAXIS will generate initial vertical stresses that are in equilibrium with the self-weight of the soil. Initial horizontal stresses, however, are calculated from the specified value of $K_0$. The value of $K_0$ for a normally consolidated soil is assumed to be related to the friction angle by Jaky's empirical expression (Brinkgreve, 2002):

$$K_0=1-\sin\varphi, \tag{1}$$

$$\sigma_{h,0}=K_0\sigma_{v,0}, \tag{2}$$

where $\varphi$ is the friction angle of soil; $K_0$ is the coefficient of lateral earth pressure at rest; $\sigma_{v,0}$ is the initial vertical stress; and $\sigma_{h,0}$ is the initial horizontal stress. In practice, two $K_0$ values can be specified, i.e., $K_{0,x}$ for the *x*-direction and $K_{0,z}$ for the *z*-direction. In this study, the $K_{0,z}$ value is equal to the $K_{0,x}$ value.

The groundwater and ground overload are not considered. Vertical model boundaries with their normal in *x*-direction (i.e., parallel to the *Y*-*Z*-plane) are fixed in *x*-direction and free in *y*- and *z*-direction. Vertical model boundaries with their normal in

$z$-direction (i.e., parallel to the $X$-$Y$ plane) are fixed in $z$-direction and free in $x$- and $y$-direction. The model bottom boundary is fixed in all directions. The "ground surface" of the model is free in all directions.

### 2.2 Mesh of model

The mesh of model is automatic in PLAXIS. The mesh around the eight lines is densified. The plane mesh of finite element is shown in Fig. 2. After the plane mesh, 3D mesh is carried on. The mesh of coupling beams and interface elements around the piles is shown in Fig. 3. The interface elements are used to simulate interaction between soil and structures (Mendonca and de Paiva, 2000; Ellis and Springman, 2001; Chen and Martin, 2002). The complete 3D mesh is shown in Fig. 4. The elements of soil are 15-node triangular prisms. The $Y$-axis is defined positive upward. The upper part of model where piles are located is densified. There are 37965 elements and 114513 nodes in all.

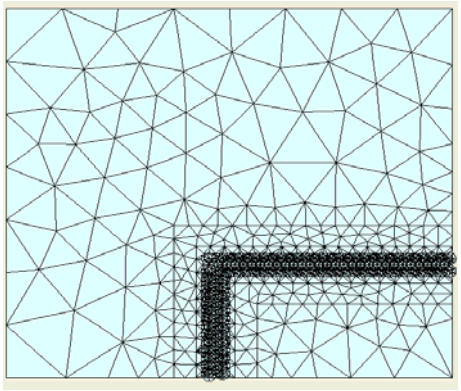

**Fig. 2 Plane mesh of model**

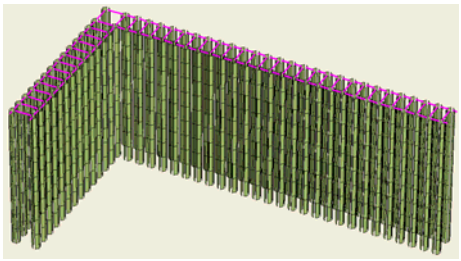

**Fig. 3 3D mesh of coupling beams and interface elements**

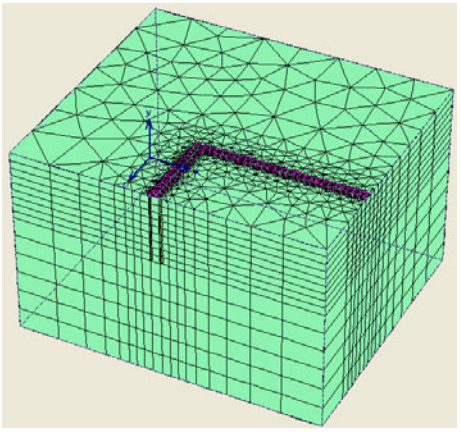

**Fig. 4 3D mesh of model**

## 3 Analysis of the model

### 3.1 Typical piles

The displacement fields of model are shown in Fig. 5. The results show that the resilience of the pit bottom and lateral displacement at the top of the piles are main deformations. Due to the large size of the model and a large quantity of the piles, few of the properties of all the piles are shown in tables or figures, but it is essential to choose the piles on special positions.

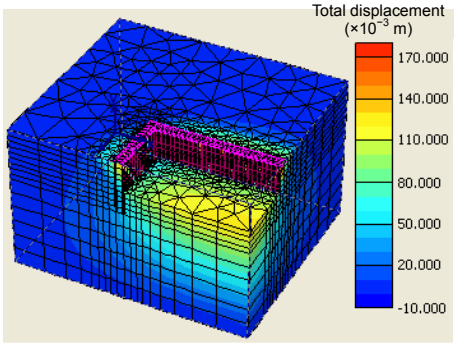


**Fig. 5 Displacement fields of model**

The lateral displacement at the top of front-row piles along the long side and short side of the foundation pit is shown in Fig. 6. The lateral displacement of the pile on the corner of the foundation pit is approximate to 0. As the distance to the corner of foundation pit increases, the lateral displacement is

observed to increase. The piles on point *A* to point *G* are chosen to be analyzed. Table 1 gives the distance to pit corner and lateral displacement at the top of piles on point *A*–point *G*. The piles on point *B*, point *C* and those on point *F*, point *E* have the same distance to the pit corner, respectively.

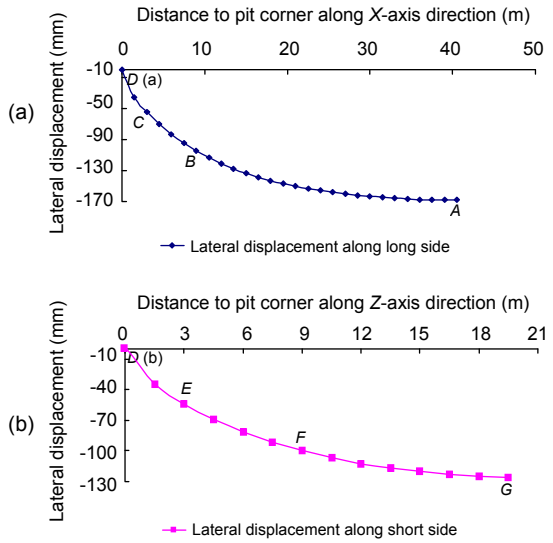


**Fig. 6 Lateral displacement at the top of front-row piles**
(a) Lateral displacement at the top of front-row piles along the long side of foundation pit; (b) Lateral displacement on the top of front-row piles along the short side of foundation pit

**Table 1 The positions of point *A*–point *G***

| Point | Distance to pit corner (m) | Lateral displacement at the top of front-row piles (cm) |
|---|---|---|
| *A* | 40.5 | 16.8 |
| *B* | 9.0 | 10.5 |
| *C* | 3.0 | 5.5 |
| *D* | 0 | 0 |
| *E* | 3.0 | 5.4 |
| *F* | 9.0 | 10.0 |
| *G* | 19.5 | 12.6 |

## 3.2 Analysis of lateral displacement

The lateral displacements of front-row and back-row piles on point *A* to point *G* are shown in Fig. 7. The lateral displacement of pile on point *D* (a) represents deformation of pile on point *D* along *Z*-axis, while the lateral displacement of pile on point *D* (b) represents deformation of pile on point *D* along *X*-axis. Above the bottom of the foundation pit, the lateral displacement of the piles on the corner of the foundation pit is very small and negligible in analysis. As the distance to the corner of the foundation pit increases, the displacement is observed to increase. For the same pile, the lateral displacement near the top of the pile is larger than that near the bottom of foundation pit. The curve shape of lateral displacement of front-row piles is concave, while the curve shape of back-row piles is convex. Under the bottom of the foundation pit, the lateral displacement of all the piles is similar and relatively small. The lateral displacement of piles on points *B*, *C*, and *D* (a) is very similar to that on points *F*, *E*, and *D* (b), respectively.

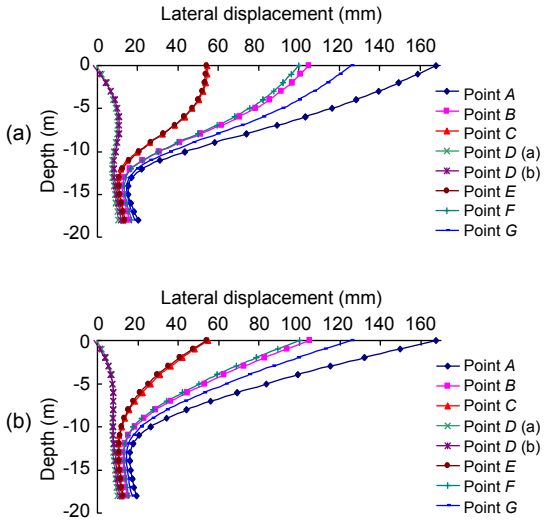


**Fig. 7 Lateral displacement of piles on point *A*–point *G***
(a) Lateral displacement of front-row piles on point *A*–point *G*; (b) Lateral displacement of back-row piles on point *A*–point *G*

## 3.3 Analysis of bending moment

The bending moments of front-row and back-row piles on point *A*–point *G* are shown in Fig. 8. The moment of pile on point *D* (a) is the moment of pile on point *D* bending around *X*-axis, while the moment of pile on point *D* (b) is the moment of pile on point *D* bending around *Z*-axis. The moment of pile is defined positive in compression at the near-pit side.

The moment of the piles on the corner of the foundation pit is very small and negligible in analysis. The moment near the top and bottom of piles is approximate to 0. The moment of front-row piles is 0 near the bottom of foundation pit. The moment of front-row piles is negative and similar above the bottom of foundation pit. The moment of front-row piles is positive under the bottom of foundation pit,

while the moment of back-row piles is always positive. As the distance to the corner of the foundation pit increases, the moment is found to increase. The moment of piles on points *B*, *C*, and *D* (a) is very similar to that on points *F*, *E*, and *D* (b), respectively.

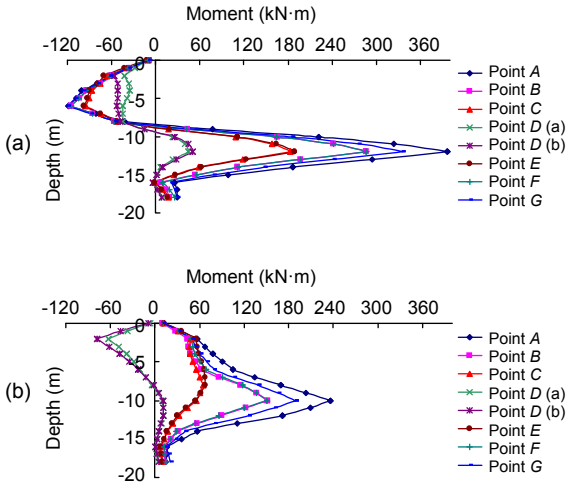


**Fig. 8 Bending moment of piles on point *A*–point *G***
(a) Moment of front-row piles on point *A*–point *G*; (b) Moment of back-row piles on point *A*–point *G*

### 3.4 Analysis of earth pressure

The earth pressures around front-row and back-row piles on point *A* to point *G* are shown in Fig. 9. Static earth pressure and the Rankine earth pressure are also drawn in Fig. 9. Static earth pressure and the Rankine earth pressure can be calculated by

$$p_0=K_0\gamma z, \tag{3}$$

$$p_a=\begin{cases}\gamma\cdot z\cdot\tan^2(45°-\varphi/2)\\ \quad -2c\cdot\tan(45°-\varphi/2),\ p_a>0,\\ 0,\ p_a\le 0,\end{cases} \tag{4}$$

$$p_p=\gamma\cdot z\cdot\tan^2(45°+\varphi/2)\\ +2c\cdot\tan(45°+\varphi/2), \tag{5}$$

where $p_0$, $p_a$ and $p_p$ are the static earth pressure, Rankine active earth pressure, and Rankine passive earth pressure, respectively; $\gamma$ is the soil density; $z$ is the depth of calculated position; and $c$ is the cohesion of soil. When the depth of calculated position is smaller than the critical depth, the Rankine active earth pressure is defined as 0.

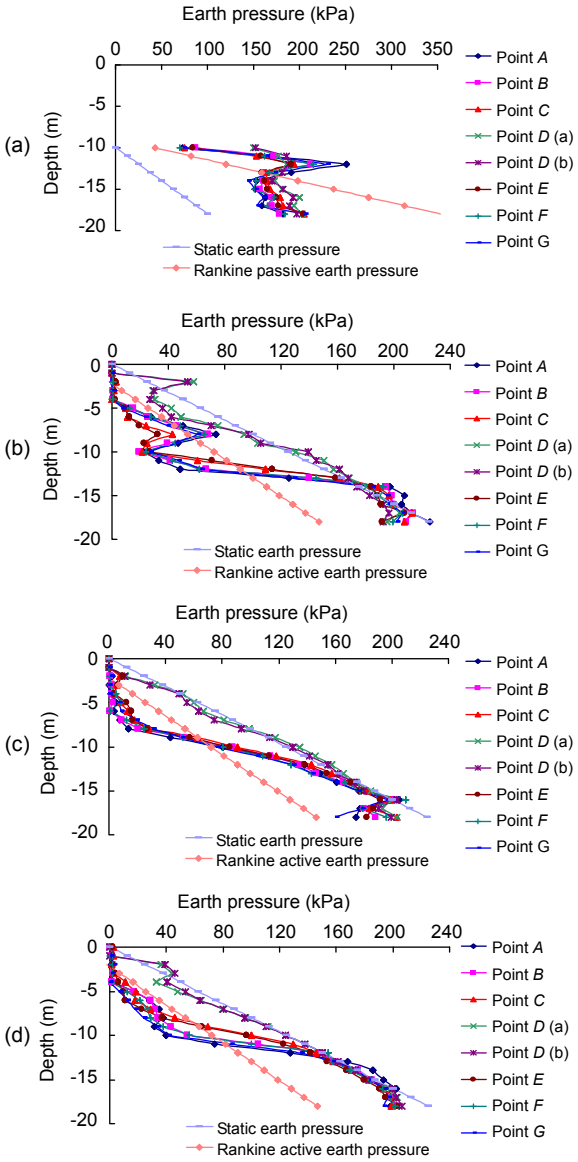


**Fig. 9 Earth pressure around piles on point *A*–point *G***
(a) Earth pressure in front of front-row piles; (b) Earth pressure in back of front-row piles; (c) Earth pressure in front of back-row piles; (d) Earth pressure in back of back-row piles

The earth pressure around pile on point *D* (a) represents lateral earth pressure around pile on point *D* along *Z*-axis, while the earth pressure around pile on point *D* (b) represents lateral earth pressure around pile on point *D* along *X*-axis. All the earth pressure in front of the front-row piles is similar. The earth pressure of the upper part of the embedded pile length is larger than the Rankine passive earth pressure, while the earth pressure of the lower part of the embedded pile length is between static earth pressure and

the Rankine passive earth pressure. The earth pressure in back of the front-row piles is similar to that around the back-row piles. Earth pressure around piles on the corner of the foundation pit is approximate to static earth pressure. The earth pressure around piles on the other positions is smaller than the Rankine active earth pressure above the bottom of foundation pit, while earth pressure is larger than the Rankine active earth pressure and approximate to static earth pressure near the bottom of the piles under the bottom of foundation pit. The earth pressure in back of the front-row piles fluctuated near the bottom of the foundation pit because of the tension of coupling beams. The earth pressure around piles on points *B*, *C*, and *D* (a) is very similar to that around piles on points *F*, *E*, and *D* (b), respectively.

## 4 Effect of length-width ratio

In parameter analyses, the middle point of the long side of the foundation pit is defined as point *A*. The lateral displacement, bending moment, and earth pressure of piles on point *A* are all the largest in the same model. The properties of piles on point *A* indicate spatial effects effectively. The behavior differences of piles on point *A* are used to reflect the influence of parameters.

Based on the basic model mentioned in Section 2, the behavior differences of double-row piles as a retaining structure are simulated through four cases with different length-width ratios. Table 2 shows the length-width ratios.

**Table 2 The length-width ratios**

| Case | Length-width ratio | Case | Length-width ratio |
|---|---|---|---|
| Case 1 | 1:1 | Case 3 | 1:5 |
| Case 2 | 1:3 | Case 4 | 1:10 |

Because the computing power is limited, the number of piles is constrained by PLAXIS 3D FOUNDATION. Keeping the length of foundation pit at 60 m, the behavior differences of piles on point *A* are simulated by decreasing the breadth of foundation pit. The 1/4 of foundation pit is chosen to be the study object due to the symmetry. The other parameters are identical with the basic model.

### 4.1 Analysis of lateral displacement

The lateral displacements of the front-row and back-row piles on point *A* are shown in Fig. 10. A decrease in length-width ratio is shown to increase the lateral displacement above the bottom of foundation pit and decrease the lateral displacement under the bottom of foundation pit. Small variations in lateral displacement are observed for remarkable variations of length-width ratio. It can be seen that the short side length of foundation pit has no significant influence on the lateral displacement of long side of foundation pit.

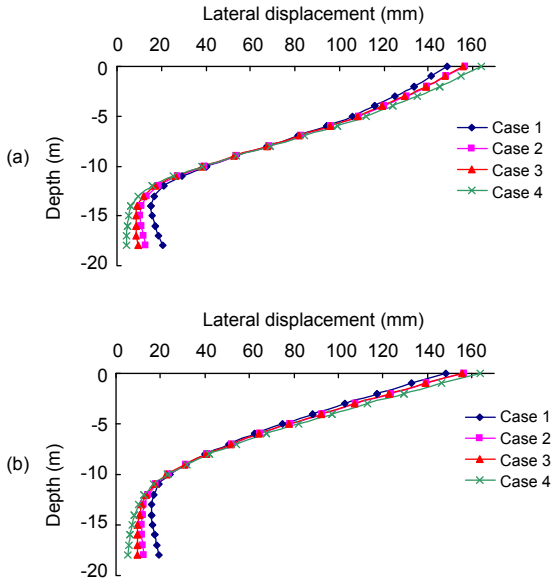


**Fig. 10 Lateral displacements of piles on point *A* with different length-width ratios**
(a) Lateral displacement of front-row pile; (b) Lateral displacement of back-row pile

### 4.2 Analysis of bending moment

The bending moments of front-row and back-row piles on point *A* are shown in Fig. 11. Variations of moment in different cases are almost the same to each other for remarkable variations of length-width ratio, which is in accord with variations of lateral displacement. It can be seen that the short side length of foundation pit has no significant effect on the moment of piles in the long side of foundation pit.

### 4.3 Analysis of earth pressure

The earth pressures around front-row and back-row piles on point *A* are shown in Fig. 12. The variations of earth pressure with remarkable variation

of length-width ratio are relatively small except for near the bottom of piles. Above all, the variation of length-width ratio has no significant influence on earth pressure in magnitude around the front-row and back-row piles.

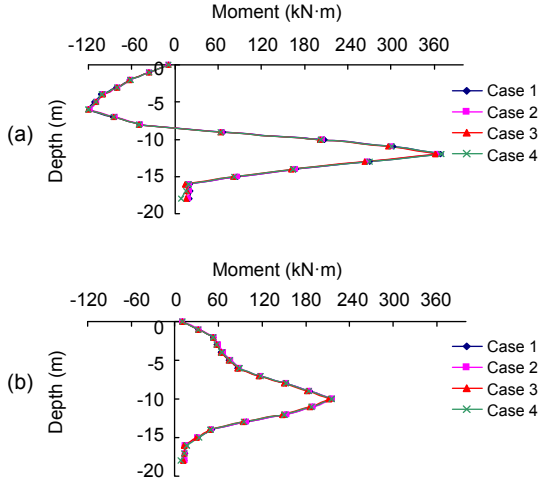


**Fig. 11 Bending moments of piles on point *A* with different length-width ratios**
(a) Moment of front-row pile; (b) Moment of back-row pile

## 5 Effect of excavation depth

Based on the basic model mentioned in Section 2, the behavior differences of double-row piles as a retaining structure are simulated through three cases with different excavation depths. Table 3 shows the excavation depths. Case 3 is the basic model. The other parameters are identical with the basic model.

### 5.1 Analysis of lateral displacement

The lateral displacements of the front-row and back-row piles on point *A* are shown in Fig. 13. The lateral displacement increases as the excavation depth increases. The lateral displacements are quite different above the bottom of foundation pit and relatively small under the bottom of foundation pit. In case 1, lateral displacement at the top of pile is approximate to 0. Lateral displacement at the bottom of pile is larger than that at the top of pile. In case 2, lateral displacement at the top of pile is approximate to that at the bottom of pile. In case 3, lateral displacement above the bottom of foundation pit is significantly larger than that in the other two cases. It can be seen that the excavation depth has a great effect on double-row piles as a retaining structure. For a cost-effective and more reliable design, it is suggested that 1/2–2/3 of pile length be chosen as the embedded depth of piles.

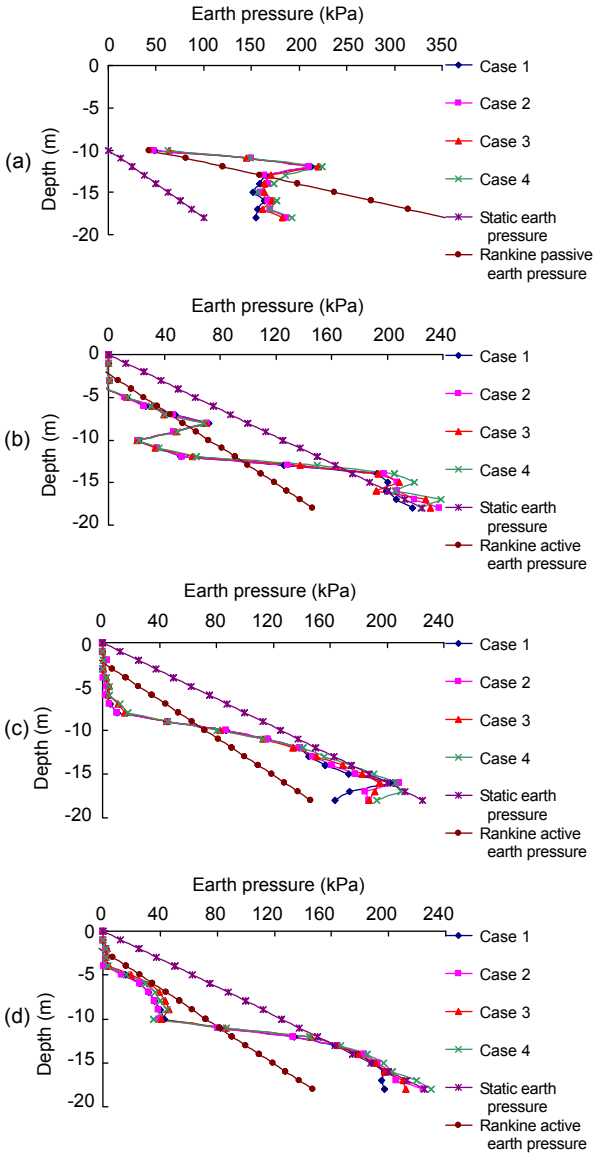


**Fig. 12 Earth pressures around piles on point *A* with different length-width ratios**
(a) Earth pressure in front of front-row pile; (b) Earth pressure in back of front-row pile; (c) Earth pressure in front of back-row pile; (d) Earth pressure in back of back-row pile

**Table 3 The excavation depths**

| Case | Excavation depth (m) |
|---|---|
| Case 1 | 6 |
| Case 2 | 8 |
| Case 3 | 10 |

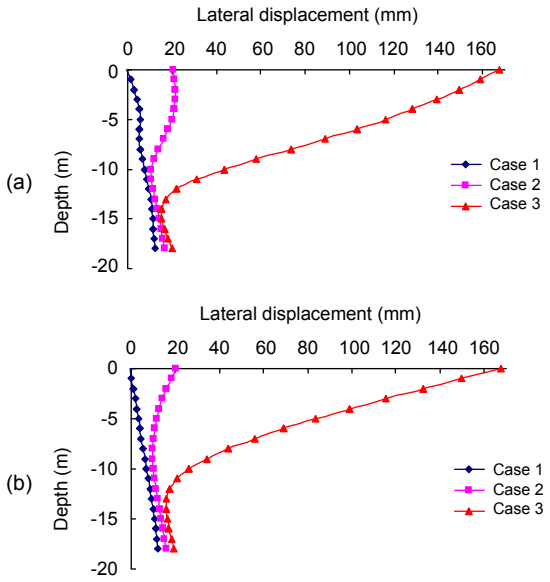


**Fig. 13 Lateral displacements of piles on point *A* with different excavation depths**
(a) Lateral displacement of front-row pile on point *A*; (b) Lateral displacement of back-row pile on point *A*

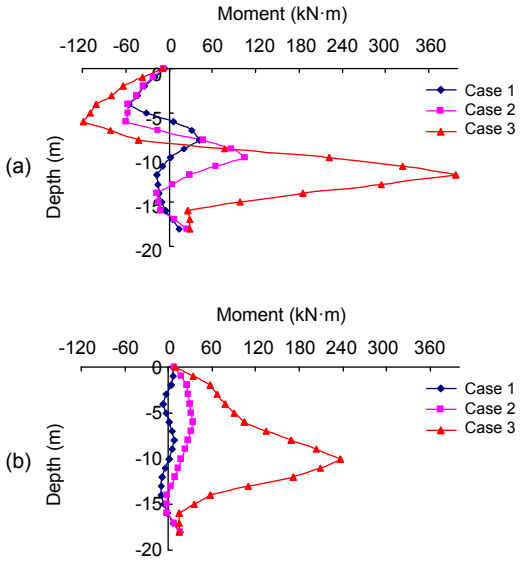


**Fig. 14 Bending moments of piles on point *A* with different excavation depths**
(a) Moment of front-row pile; (b) Moment of back-row pile

### 5.2 Analysis of bending moment

The bending moments of the front-row and back-row piles on point *A* are shown in Fig. 14. The bending moment increases as the excavation depth increases. In case 1 and case 2, because the pit resilience is the main deformation, the moment of front-row piles is negative between the bottom of foundation pit and the bottom of piles. In case 1, bending moment of back-row pile is very small, and its sign (positive or negative) may be changed easily due to many factors, such as the self-weight of soil between rows, pit resilience, and tension of coupling beams. In general, the variation of moment consists with the variation of lateral displacement.

### 5.3 Analysis of earth pressure

The earth pressures around the front-row and back-row piles on point *A* are shown in Fig. 15. The earth pressure follows a similar trend with the variation of excavation depth. The variation of earth pressure is the most significant and the least significant in case 3 and case 1, respectively. The earth pressure in case 3 is the largest in Fig. 15a, and the smallest in Fig. 15b, Fig. 15c and Fig. 15d. In general, the variation of excavation depth influences the earth pressure in magnitude around the front-row and back-row piles to some extent.

## 6 Effect of distance between rows

Based on the basic model mentioned in Section 2, the behavior differences of double-row piles as a retaining structure are simulated through five cases with different distances between rows. Table 4 shows the distances between rows. Case 2 is the basic model. *d* is the diameter of the piles. The other parameters are identical with the basic model.

### 6.1 Analysis of lateral displacement

The lateral displacements of the front-row and back-row piles on point *A* are shown in Fig. 16. The lateral displacement decreases with increasing distance between rows. Above the bottom of foundation pit, lateral displacements are quite different. In case 1 and case 2, the curves of lateral displacements are almost parallel. In case 4 and case 5, the lateral displacement at the top of front-row piles is not the largest owing to the tension of coupling beams. The largest lateral displacement occurs between the top of piles and the bottom of foundation pit. There is a significant difference in lateral displacement between front-row piles and back-row piles. Under the bottom of foundation pit, all the lateral displacements are relatively small and similar. Judged by lateral displacement, increasing the distance between rows is

favorable to double-row piles as a retaining structure. 3*d*–6*d* is suggested as the distance between rows for a more cost-effective and more reliable design.

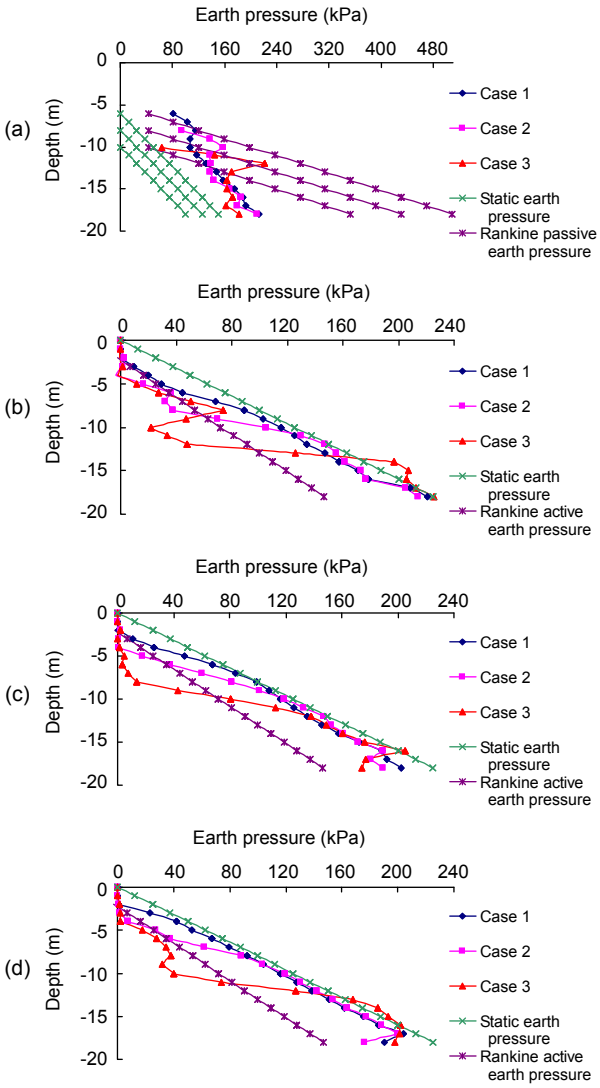


**Fig. 15 Earth pressures around piles on point *A* with different excavation depths**
(a) Earth pressure in front of front-row pile; (b) Earth pressure in back of front-row pile; (c) Earth pressure in front of back-row pile; (d) Earth pressure in back of back-row pile

**Table 4 The distances between rows**

| Case | Distance between rows (m) | Case | Distance between rows (m) |
|---|---|---|---|
| Case 1 | 1.5 (2.5*d*) | Case 4 | 7.0 (11.7*d*) |
| Case 2 | 2.5 (4.2*d*) | Case 5 | 10.0 (16.7*d*) |
| Case 3 | 4.5 (7.5*d*) | | |

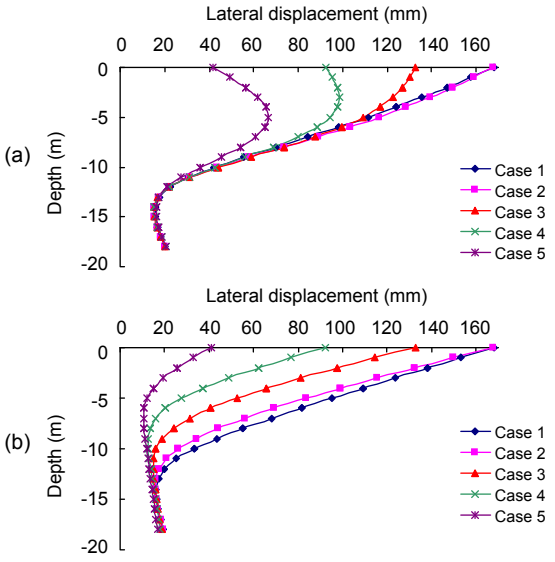


**Fig. 16 Lateral displacements of piles on point *A* with different distances between rows**
(a) Lateral displacement of front-row pile; (b) Lateral displacement of back-row pile

## 6.2 Analysis of bending moment

The bending moments of the front-row and back-row piles on point *A* are shown in Fig. 17. Above the bottom of foundation pit, the moment of front-row piles increases with increasing distance between rows. In case 4 and case 5, the curves of moments of front-row piles are almost parallel. Under the bottom of foundation pit, the moment of front-row pile in case 5 is a little smaller than that in the other cases. Thus, in case 5, the largest negative moment of front-row pile above the bottom of foundation pit is approximate to the largest positive moment under the bottom of foundation pit, which is very favorable to the structures.

The largest moment of back-row pile in case 5 is also the smallest. In the other cases, the largest moments of back-row piles are similar. However, the position where the largest moment of back-row pile occurs is elevated with increasing distance between rows. In general, increasing distance between rows has no unfavorable effects on the moment of piles.

## 6.3 Analysis of earth pressure

The earth pressures around the front-row and back-row piles on point *A* are shown in Fig. 18. The earth pressure follows a similar trend with the

variation of distance between rows. In all cases, the curves of earth pressure around front-row piles are almost parallel. The earth pressure around back-row pile increases with increasing distance between rows. In general, the difference in distance between rows has certain influence on earth pressure in magnitude around the back-row piles. The variation of earth pressure has a good agreement with those of the displacement and the moment.

## 7 Effect of diameter of piles

Based on the basic model mentioned in Section 2, the behavior differences of double-row piles as a retaining structure are simulated through three cases with different diameters of the piles. Table 5 shows the diameters of the piles. Case 1 is the basic model. The other parameters are identical with the basic model.

### 7.1 Analysis of lateral displacement

The lateral displacements of the front-row and back-row piles on point *A* are shown in Fig. 19.

As the diameter of piles increases, the lateral displacement is found to decrease. Above the bottom of foundation pit, lateral displacements are quite different, while under the bottom of foundation pit, lateral displacements are relatively small and similar. In

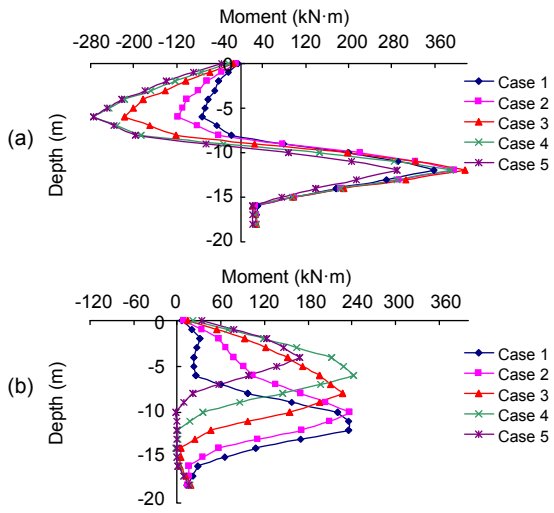


**Fig. 17 Bending moments of piles on point *A* with different distances between rows**
(a) Moment of front-row pile; (b) Moment of back-row pile

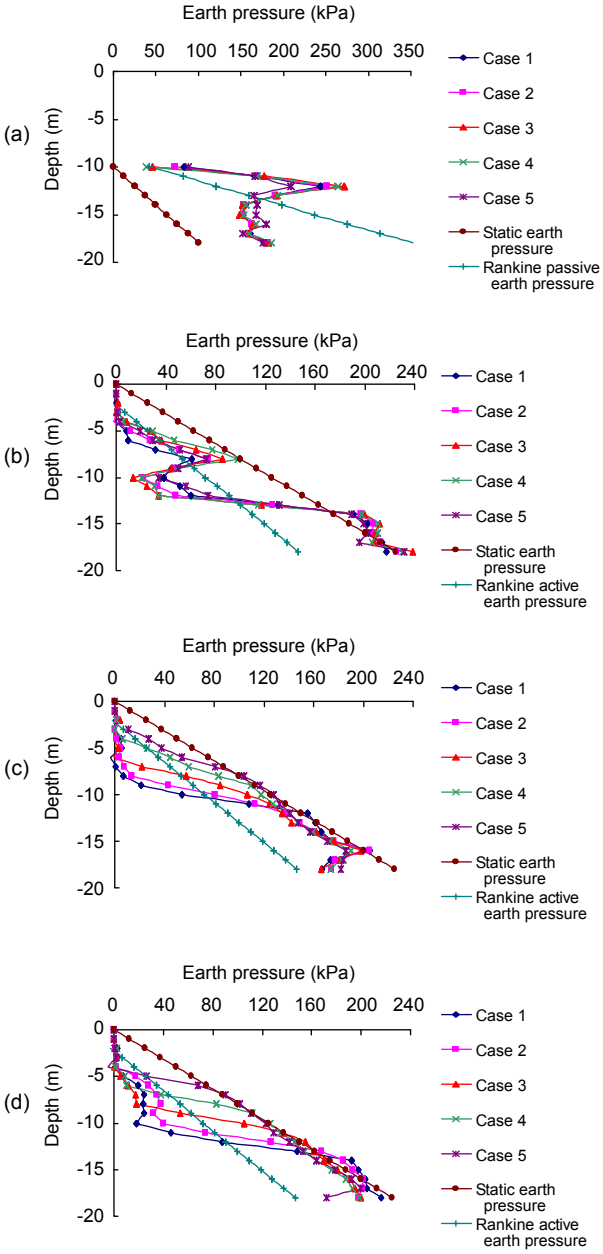


**Fig. 18 Earth pressures around piles on point *A* with different distances between rows**
(a) Earth pressure in front of front-row pile; (b) Earth pressure in back of front-row pile; (c) Earth pressure in front of back-row pile; (d) Earth pressure in back of back-row pile

**Table 5 The diameters of the piles**

| Case | Diameter of piles (m) |
|---|---|
| Case 1 | 0.6 |
| Case 2 | 0.8 |
| Case 3 | 1.0 |

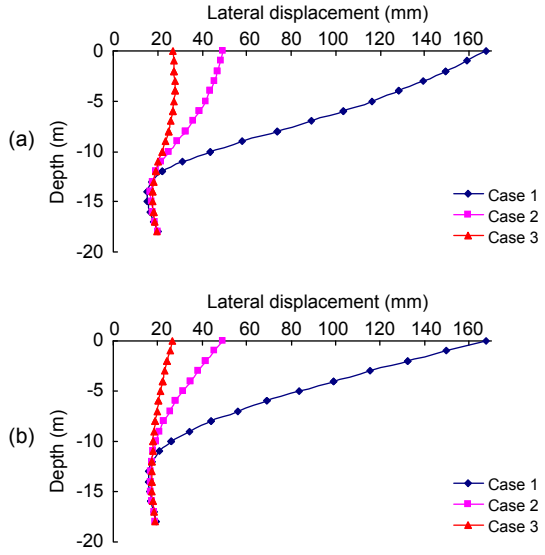


**Fig. 19 Lateral displacements of piles on point *A* with different diameters of piles**
(a) Lateral displacement of front-row pile; (b) Lateral displacement of back-row pile

case 3, lateral displacement at the top of pile is approximate to that at the bottom of pile. In case 1, lateral displacement above the bottom of foundation pit is significantly larger than that in the other two cases. It can be observed that the diameter of the piles has a great influence on double-row piles as a retaining structure.

### 7.2 Analysis of bending moment

The bending moments of the front-row and back-row piles on point *A* are shown in Fig. 20. Above the bottom of foundation pit, the moment of the front-row pile in case 3 is much larger than that in the other two cases. The curves of moments in case 1 and case 2 are almost parallel. Under the bottom of foundation pit, the moment of front-row pile in case 1 is the largest. The largest moments of front-row piles in case 2 and case 3 are similar.

As the diameter of piles increases, the moment of back-row piles is found to decrease. The largest moment of back-row piles appears at the bottom of foundation pit in case 1 and case 2, while the largest moment of back-row pile occurs between the bottom of foundation pit and the bottom of pile in case 3. With an increase in diameter of piles, a certain bending moment is gradually generated at the bottom of piles due to the effect of pit resilience. Based on an overall consideration of displacement and moment, it is suggested that 0.6–1.2 m and 2*d*–2.5*d* be chosen as diameter of piles and distance between piles, respectively.

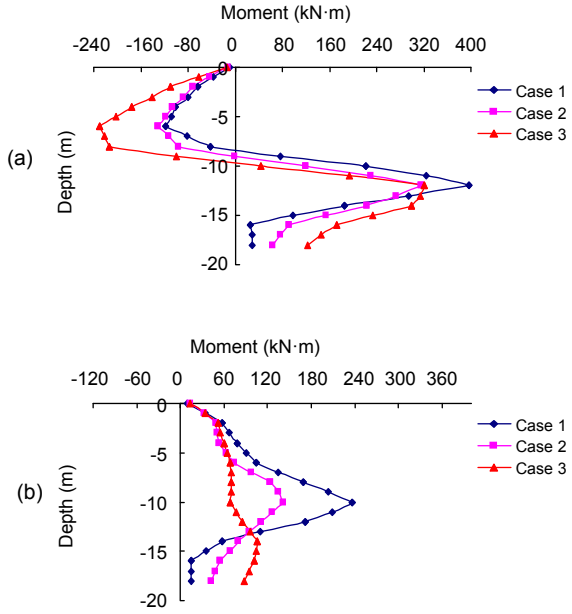


**Fig. 20 Bending moments of piles on point *A* with different diameters of piles**
(a) Moment of front-row pile; (b) Moment of back-row pile

### 7.3 Analysis of earth pressure

The earth pressures around the front-row and back-row piles on point *A* are shown in Fig. 21. The earth pressure follows a similar trend with different diameters of piles. In case 1, the variation of earth pressure is the most significant. For case 2 and case 3, the curves of earth pressure are almost parallel. The earth pressure around back-row pile in case 1 is a little smaller than that in the other two cases. In general, the variation of diameter of piles has no obvious influence on earth pressure in magnitude around the front-row and back-row piles.

## 8 Conclusions

Based on the results of this study, the following conclusions can be drawn.

1. The lateral displacement of the front-row piles is larger than that of the back-row piles. Thus, the

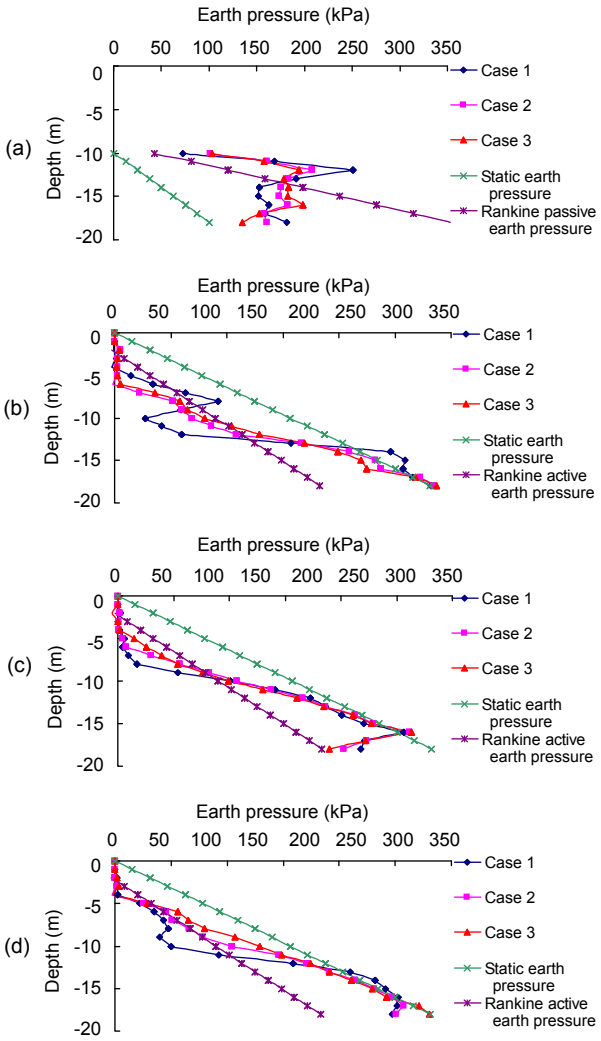


**Fig. 21 Earth pressures around piles on point *A* with different diameters of piles**

(a) Earth pressure in front of front-row pile; (b) Earth pressure in back of front-row pile; (c) Earth pressure in front of back-row pile; (d) Earth pressure in back of back-row pile

distance between rows after deformation is larger than that in the initial state. This means that the restriction effect on soil between rows has decreased after deformation. Above the bottom of foundation pit, earth pressure in back of front-row piles and in front of back-row piles is approximate to the Rankine active earth pressure. It is suggested that the earth pressure between the rows above the pit bottom is close to active earth pressure, while under the pit bottom, earth pressure between the rows is close to static earth pressure.

2. The Rankine active earth pressure is larger than calculated active earth pressure in the finite element method, while it is smaller than calculated passive earth pressure in the finite element method.

3. The short side length of foundation pit has no significant effect on the long side of foundation pit. When the foundation pit is large enough, the interaction between long side and short side of foundation pit can be neglected in analysis.

4. If two piles in long side and short side of foundation pit have the same distance to the corner, they would have approximately the same lateral displacement, bending moment, and earth pressure.

5. If excavation depth is small, pit resilience may be the main deformation. Lateral displacement at the bottom of piles could be larger than that at the top of piles. As the excavation depth increases, the lateral displacement above pit bottom increases. 1/2–2/3 of pile length as embedded depth of piles is suggested.

6. With increasing distance between rows the lateral displacement decreases. An increasing distance between rows has no unfavorable effects on the moment of piles. 3*d*–6*d* as distance between rows is suggested, where *d* is the diameter of the piles.

7. As the diameter of piles increases, the lateral displacement is observed to decrease. With the increasing diameter of piles, the moment of piles shows an irregular variation. 0.6–1.2 m and 2*d*–2.5*d* are suggested as diameter of piles and distance between piles, respectively.

## References

Brinkgreve, R.B.J., 2002. PLAXIS-Finite Element Code for Soil and Rock Analyses, 2D-Version 8. A.A. Balkema, Rotterdam, the Netherlands.

Chen, C.Y., Martin, G.R., 2002. Soil-structure interaction for landslide stabilizing piles. *Computers and Geotechnics*, **29**(5):363-386. [doi:10.1016/S0266-352X(01)00035-0]

Ellis, E.A., Springman, S.M., 2001. Modelling of soil-structure interaction for a piled bridge abutment in plane strain FEM analyses. *Computers and Geotechnics*, **28**(2):79-98. [doi:10.1016/S0266-352X(00)00025-2]

He, Y., Yang, B., Jin, B., Li, R., Tan, Y., Wang, T., 1996. A study on the test and calculation of double-row fender piles. *Journal of Building Structures*, **17**(2):58-66 (in Chinese).

Mendonca, A.V., de Paiva, J.B., 2000. A boundary element method for the static analysis of raft foundations on piles. *Engineering Analysis with Boundary Elements*, **24**(3): 237-247. [doi:10.1016/S0955-7997(00)00002-3]

Neher, H.P., Wehnert, M., Bonnier, P.G., 2001. An Evaluation of Soft Soil Models Based on Trial Embankments. Proceedings of the Tenth International Conference on

Computer Methods and Advances in Geomechanics, Tucson, Arizona, USA. A.A. Balkema, Rotterdam, the Netherlands, p.373-378.

Sun, Y., 2008. Research on mechanism and application of the double-row retaining piles for deep pits. *Building Science*, **24**(11):60-65 (in Chinese).

Wu, G., 2006. Theoretical Analysis and Numerical Calculation of Retaining Structure with Double-Row Piles of Deep Foundation Pit. MS Thesis, Beijing Jiaotong University, Beijing, China (in Chinese).

Yang, J., 2005. FEA of Double-Row Piles Considering the Dimension Effects. MS Thesis, Tianjin University, Tianjin, China (in Chinese).

Zheng, G., Li, X., Liu, C., Gao, X., 2004. Analysis of double-row piles in consideration of the pile-soil interaction. *Journal of Building Structures*, **25**(1):99-106 (in Chinese).